Spectral Theory of Microwave Holographic Image Formation

A. Popov, I. Prokopovich, V. Kopeikin, D. Edemskij

Pushkov Institute of Terrestrial Magnetism, Ionosphere and Radio Wave Propagation

IZMIRAN, 142190, Troitsk, Moscow, Russia. popov@izmiran.ru

Abstract— The capabilities of subsurface microwave holography are limited by mutually contradicting factors, such as penetration depth, surface reflection, and spatial resolution. As a result of the trade-off, the wavelength at the operating frequency is comparable to the typical target sizes and is not small compared with the antenna array dimensions and probing range. In order to comprehend microwave image formation by a planar holographic antenna array we apply Fresnel-Kirchhoff diffraction theory uniformly treating target illumination, incident wave scattering, holographic data acquisition, and object reconstruction by means of numerical wave front conversion. Within the framework of narrow-angle diffraction model we derive an integral operator directly transforming the planar test object into its diffraction-limited image. The action of this operator is readily revealed by applying Fourier transform with respect to the transversal coordinates: it cuts from the target spatial spectrum a rectangular segment centered according to the illumination angle. The theory shows that for a successful object reconstruction the acquired rectangle must cover the significant part of the target spatial spectrum. If the antenna aperture is too small to meet this condition, synthetic aperture approach can be successfully used. Such a multiview-multistatic measurement scheme realized by moving the radiator around the fixed receiver antenna array may considerably improve the radar imaging performance - cf. [1]. This conclusion was confirmed by numerical simulation and physical experiment.

Index Terms— microwave holography, object reconstruction.

I. INTRODUCTION

One of the basic difficulties in subsurface microwave holography consists in substantial distortion of the image and its dependence on mutual positions of the object, holographic antenna and radiator. The decisive factor here is the loss of a considerable part of the information about the object contained in the angular spectrum of the scattered radiation [2]. For a careful study of this effect, occurring also in free space, we have performed a series of physical experiments with a planar test object, their numerical simulation and theoretical analysis.
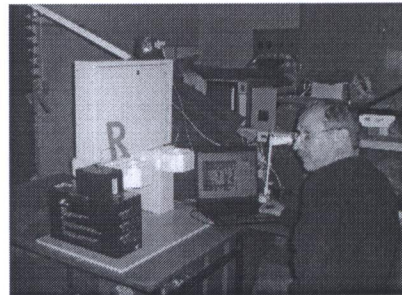

Fig. 1. Experimental setup and a copy of the test object

Our primary goal was to test a prototype of holographic subsurface radar [3] provided by JSC VNIISMI [4] – see Fig. 1. As a test object, we chose a freely suspended metal stencil of letter "R", 10x15 cm wide, illuminated by coherent microwave radiation. Amplitude and phase distribution of the backscattered radiation in the receiver plane $z = 0$ was registered by a rectangular multi-element antenna array. Object reconstruction was performed by the wave front conversion procedure [5,6] based on Fresnel-Kirchhoff approximation [7]. We studied the image quality and the possibility to recover the true object shape, depending on distance and the radiator position. A 10 GHz radiator horn antenna was placed at different points on the receiver antenna array perimeter. Experimental results – radio images of the test object placed at $l = 35$ cm from the holographic receiver array, are shown in the left column of Fig. 2.

The results of numerical simulation – amplitude distribution of the inverted wave in the object plane $z = l$, are presented in the right column of Fig.2. A good agreement between experimental and simulated images confirms the applicability of the Kirchhoff diffraction theory to the qualitative description of both scattering process and object reconstruction. At the same time, the obtained images are far from being a good copy of the object. Qualitative analysis of the images also reveals the correlation between the image shape and the reflected wave phase distribution over the object area. The dependence of Fresnel zone configuration on the radiator position suggests the idea of using multi-directional illumination for
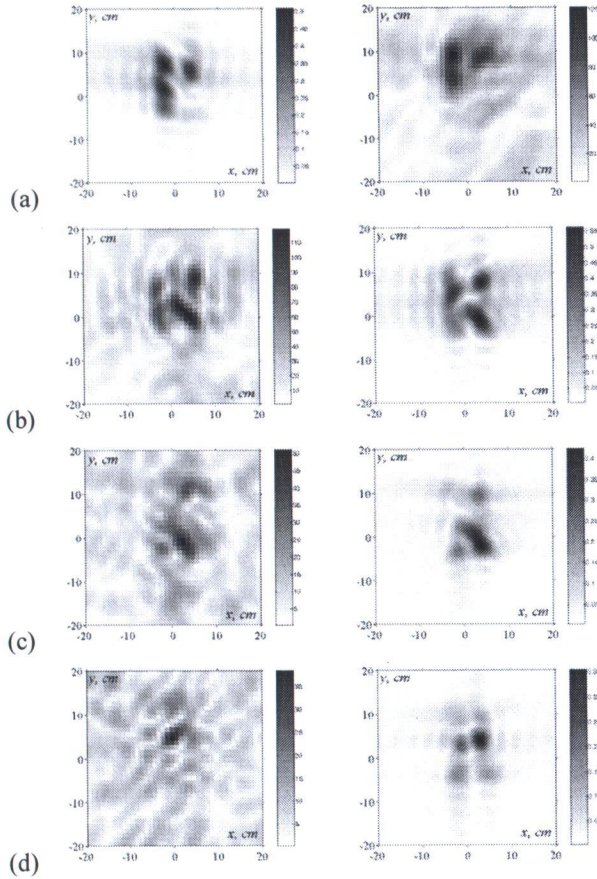
(a)

(b)

(c)

(d)

Fig. 2. Test object images for different radiator positions (x*, y*, z*): (a) left-top (-30, 15, -5) cm; b) right-top (30, 15, -5) cm; (c) left-bottom (-30, -15, -5) cm; (d) right-bottom (30, -15, -5) cm. Left column: experiment; right column: numerical simulation.

improving the radar portrait of the object. The simplest way is just to add the amplitudes or intensities of the images obtained with different illumination directions. The result of such addition is shown in Fig. 3. One can see that such a synthesized image gives a better notion of the object shape.

In what follows we demonstrate that the image quality can be further improved by coherent superposition of holograms obtained with different illumination bearings.

II. SPECTRAL THEORY OF IMAGE FORMATION

According to Fresnel-Kirchhoff theory [7], the scattered wave produced by a planar reflecting object illuminated by an incident plane wave is given by the integral:

$$E_s(x,y,z) = \frac{k}{2\pi i}\int_{-\infty}^{\infty}\int_{-\infty}^{\infty}\frac{e^{ikR}}{R}E(\xi,\eta,l)d\xi d\eta \ . \tag{1}$$

Here, $E(\xi,\eta,l) = f(\xi,\eta)\exp[ik(x\sin\alpha_0 + y\sin\beta_0)]$, $k = \omega/c$ is the wave number, and $f(\xi,\eta)$ - is the reflection
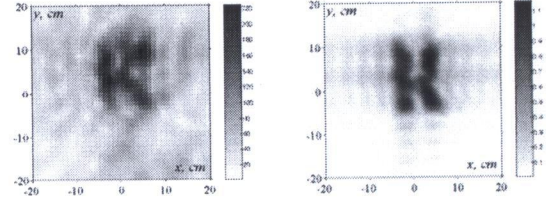

Fig. 3. Object reconstruction by adding the inverted wave field amplitudes for different radiator positions presented in Fig.2 – experiment and simulation.

coefficient, considered to be constant over the target area.

Within narrow-angle approximation:

$$R \approx l - z + \frac{(\xi-x)^2 + (\eta-y)^2}{2(l-z)} \tag{2}$$

the microwave hologram (amplitude and phase distribution of the scattered wave field $h(x_0,y_0) \equiv E_s(x_0,y_0,0)$ recorded in the receiver antenna aperture $z = 0$ $|x_0| < a$, $|y_0| < b$) has the following form

$$h(x_0,y_0) = e^{ikl}\frac{k}{2\pi i l}\int_{-\infty}^{\infty}\int_{-\infty}^{\infty}E(x,y,l)e^{ik\frac{(\xi-x)^2+(\eta-y)^2}{2l}}d\xi d\eta \tag{3}$$

Object reconstruction is performed using «anti-Kirchhoff» formula [6]:

$$g(x,y) \equiv E_r(x,y,l) = \frac{k}{2\pi i}\int_{-a}^{a}\int_{-b}^{b}h(x_0,y_0)\frac{e^{-ikR_0}}{R_0}dx_0 dy_0 \ , \tag{4}$$

where $R_0 \approx l + \frac{(x-x_0)^2 + (y-y_0)^2}{2l}$. Denoting

$$\tilde{f}(\xi,\eta) = f(\xi,\eta)e^{ik\frac{\xi^2+\eta^2}{2l}}, \qquad \tilde{g}(x,y) = g(x,y)e^{ik\frac{x^2+y^2}{2l}}, \quad \text{we}$$

obtain after standard derivation

$$\tilde{g} = \frac{1}{\pi^2}\int_{-\infty}^{\infty}\int_{-\infty}^{\infty}\tilde{f}(\xi,\eta)e^{i(p_0\xi+q_0\eta)}\frac{\sin\mu(\xi-x)}{\xi-x}\cdot\frac{\sin\nu(\eta-y)}{\eta-y}d\xi d\eta$$

$$\mu = \frac{ka}{l}, \ \nu = \frac{kb}{l}, \ p_0 = k\sin\alpha_0, \ q_0 = k\sin\beta_0 \tag{5}$$

This formula explicitly represents transformation of a planar test object $f(x,y)$ into its holographic image $g(x,y)$, with given antenna parameters, location range and incident wave direction.

For the unknown function $f(x,y)$, the above formula yields an integral equation. Its solution, corresponding to perfect object reconstruction, requires strong analytical implications [8]. The action of the integral operator becomes obvious after applying Fourier transform:
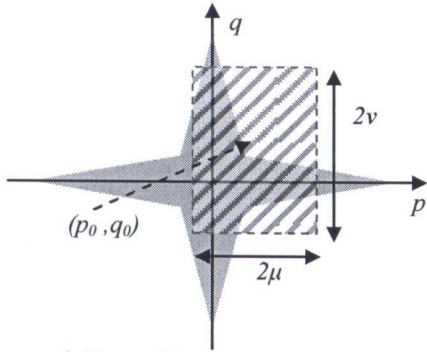
Fig. 4. Diagram of object spatial spectrum and antenna spectral window.

Fig. 6. Test object and its spatial spectrum.

$$\tilde{F}(p,q) = \int_{-\infty}^{\infty} \int_{-\infty}^{\infty} \tilde{f}(x,y) e^{-i(px+qy)} dx dy,$$

$$\tilde{G}(p,q) = \int_{-\infty}^{\infty} \int_{-\infty}^{\infty} \tilde{g}(x,y) e^{-i(px+qy)} dx dy \qquad (6)$$

converting the convolution integral (5) into a product.

$$\tilde{G}(p,q) = \tilde{F}(p-p_0, q-q_0) \cdot \Pi_\mu(p) \cdot \Pi_\nu(q) \qquad (7)$$

where $\Pi_\mu(p) \cdot \Pi_\nu(q)$ - step function equal to unity inside the rectangle $|p| < \mu$, $|q| < \nu$ and to zero outside it. For a given wavelength $\lambda = \dfrac{2\pi}{k}$, antenna aperture (a,b) and probing range l, microwave hologram represents a rectangular portion of the modified spatial object spectrum $\tilde{F}(p,q)$, determined by the incident wave vector (p_0, q_0) and spectral window half-width $\mu = \dfrac{ka}{l}$, $\nu = \dfrac{kb}{l}$:

$$p_0 - \mu < p < p_0 + \mu, \quad q_0 - \nu < q < q_0 + \nu, \qquad (8)$$

see Fig.4. The shift $p \to p + p_0$, $q \to q + q_0$, where $p_0 = k \sin\alpha_0$, $q_0 = k \sin\beta_0$, is defined by the incidence angle of the illuminating plane wave. Within geometrical optics approximation, the reflected wave angular spectrum merely repeats the spatial spectrum of the target reflection coefficient; the modified spectrum definition

$$\tilde{F}(p,q) = \int_{-\infty}^{\infty} \int_{-\infty}^{\infty} f(x,y) \exp\left[i\left(k \frac{x^2+y^2}{2l} + px + qy \right) \right] dx dy \quad (9)$$

takes into account diffraction effects.

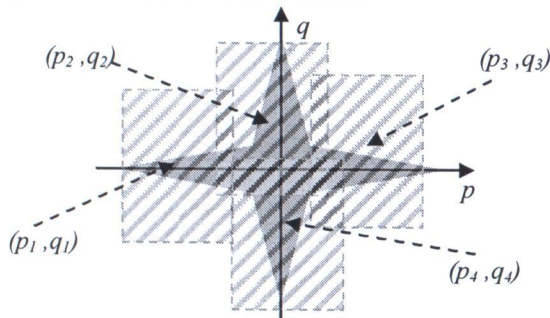Fig. 5. Schematic picture of multidirectional object illumination.
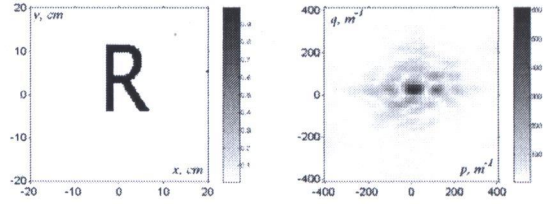
From the practical point of view, the recipe for getting a good image is obvious: a significant part of the scattered radiation must fall into the holographic antenna aperture and not be blurred by diffraction. This goal can be achieved by enlarging antenna aperture, increasing operating frequency or reducing the distance to the object, which has been done by coherent holographic scanning in [9]. If the operating frequency and antenna dimensions are fixed and the probing distance can not be reduced, the image quality can be improved by means of coherent multi-position object illumination allowing one to register all the significant part of the scattered radiation – see Fig. 5.

III. NUMERICAL SIMULATION

In order to illustrate the above results let us analyze from the spectral point of view the image formation of the chosen test object. Its spatial spectrum is presented in the right part of Fig.6. Holographic images of the test object calculated by the spectral method for the probing distance $l = 50$ cm and for different illumination directions are displayed in the left column of Fig. 7. In the right column, the portion of the spatial object spectrum falling into the antenna aperture for the corresponding radiator position is shown.

Comparing the spectral patterns from the right column with the full spatial spectrum of Fig. 6 we see how the truncation affects the holographic image, making the object almost unrecognizable. In accordance with the spectral theory, coherent superposition of the presented above holograms may radically improve the image. The upper part of Fig. 8 confirms this prediction: although each of the blurred images of Fig. 7 is far from representing true object shape - Fig. 8(a), the quality of the synthetic coherent portrait Fig. 8(b) is quite satisfactory from the practical point of view. It is fully consistent with the developed spectral theory, for the synthesized spectral chart shown in Fig. 8(c) covers a considerable part of the object spatial spectrum. The remaining image defects are due to the gaps in the upper corners of the spectral pattern and can be removed by adding holographic data obtained with other illumination directions.
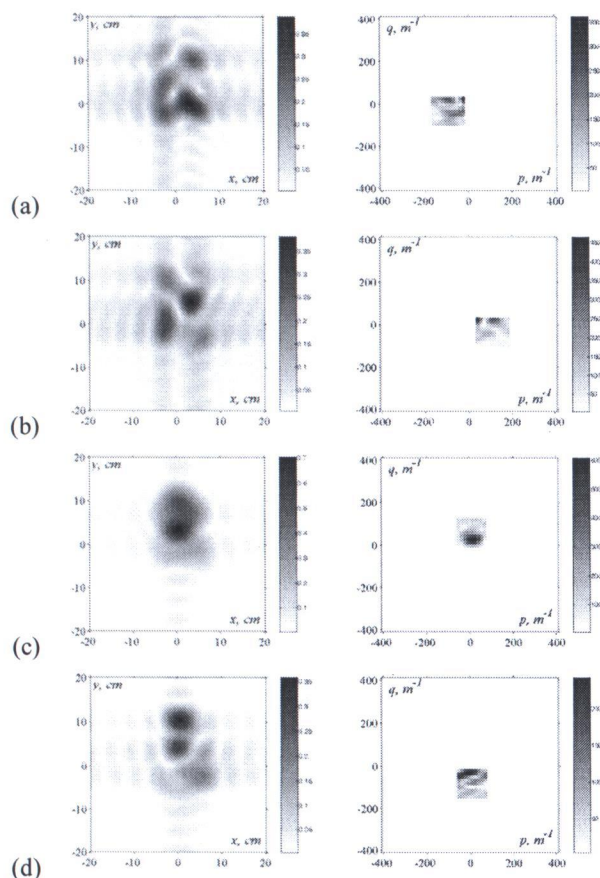
(a)

(b)

(c)

(d)

Fig. 7. Left column: holographic images of the test object for different illumination angles. (a) from left: $(\mathrm{tg}\,\alpha_0, \mathrm{tg}\,\beta_0) = (30/50, 10/50)$;

(b) from right: (-30/50, 10/50); (c) from above: (0, -10/50); (d) from below: (0, 25/50). Right column: part of spatial spectrum falling into antenna angular spectral window from $l = 50$ cm.

IV. CONCLUSION

Spectral analysis quantitatively describes the speckle structure distorting microwave holographic images of a test object. It allows one to choose optimal illumination conditions and to improve the image quality by means of coherent multiview measurements.

ACKNOWLEDGMENT

(a)   (b)
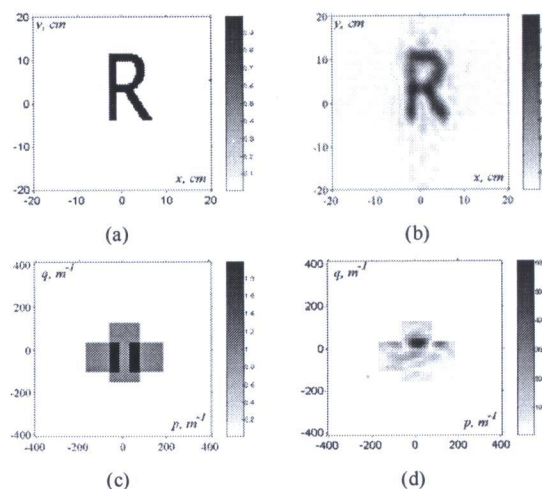
(c)   (d)

Fig. 8. (a) test object under study; (b) coherent superposition of four holographic patterns shown in Fig. 7; (c) synthesized spectral coverage map; (d) synthesized image spatial spectrum/

REFERENCES

[1] R. Persico, R. Bernini, and F. Soldovieri, "The role of measurement configuration in inverse scattering from buried objects under the Born approximation", IEEE Transactions on Antennas and Propagation, vol. 53, No 6, pp.1875 − 1887, 2005.

[2] D. Pommet, R. A. Marr, U. H. WW. Lammers, R. W. McGahan, J. B. Morris, and M. A. Fiddy, "Imaging using limited-angle backscattered data", IEEE Antennas and Propagation Magazine, vol. 39, No 2, pp.19 − 22, 1997.

[3] V. Kopeikin and A. Popov, "Design concepts of the holographic subsurface radar", Radiophysics and Quantum Electronics, vol. 43. No 3, pp. 202 − 210, 2000.

[4] http://www.geo-radar.ru.

[5] A. Popov and V. Vinogradov, "Focused Gaussian beams in the problem of holographic imaging", IEEE Transactions on Antennas and Propagation, vol. 50, No 9, pp.1236 − 1244, 2002.

[6] A. Popov, V. Kopeikin, V. Vinogradov, and S. Zapunidi, "Reconstruction algorithms and experiments with a prototype of holographic subsurface radar", in Proc. of 4th International Conf. on Antennas Theory and Techniques, Sevastopol, Ukraine. vol. 2, pp. 561 − 563, IEEE, 2003.

[7] M. Born and E. Wolf. Principles of Optics: Electromagnetic Theory of Propagation, Interference and Diffraction of Light. Cambridge University Press, 1999.

[8] E. C. Titchmarsh. Introduction to the Theory of Fourier Integrals. Chelsea Publishing Company, 1986.

[9] V. Razevig, S. Ivashov, I. Vasiliev, and A. Zhuravlev, "Comparison of different methods for reconstruction of microwave hologram recovded by the subsurface radar", in Proc of 14th Conf. on Ground Penetrating Radar, vol. 2, pp. 335-339, Shanghai, China, 2012.